Controlled synthesis of pure and highly dispersive Cu(II), Cu(I), and Cu(0)/MCM-41 with $Cu[OCHMeCH_2NMe_2]_2$/MCM-41 as precursor

Guoying Zhang, Jinlin Long, Xuxu Wang,* Wenxin Dai, Zhaohui Li, Ling Wu and Xianzhi Fu*

Received (in Gainesville, FL, USA) 31st March 2009, Accepted 15th June 2009
First published as an Advance Article on the web 20th July 2009
DOI: 10.1039/b906352h

Cu(II)/MCM-41, Cu(I)/MCM-41 and Cu(0)/MCM-41 materials were prepared with $Cu[OCHMeCH_2NMe_2]_2$/MCM-41 as precursor under controlled conditions. The states of copper on the resulting samples were characterized by temperature programmed reduction (TPR), UV-Vis diffuse reflectance spectroscopy (UV-Vis DRS), X-ray photoelectron spectroscopy (XPS), photoluminescence spectroscopy (PL), infrared spectroscopy (FTIR) of NO and CO adsorption, X-ray diffraction (XRD), and N_2 adsorption. It was shown that pure Cu(II)/MCM-41 can be acquired by calcining $Cu[OCHMeCH_2NMe_2]_2$/MCM-41 in pure oxygen at 573 K. Pure Cu(I)/MCM-41 can be obtained by reducing the as-prepared Cu(II)/MCM-41 in a CO/He atmosphere at 473 K, while pure Cu(0)/MCM-41 can be obtained *via* reduction of the Cu(II)/MCM-41 in a CO/He atmosphere at 673 K. The Cu(II)–O and Cu(I)–O species were showed to be highly dispersed on the surface of MCM-41 as isolated sites. The study provides an alternative method for the preparation of pure copper metal or copper oxide supported materials.

Introduction

Metal-supporting zeolite molecular sieves are widely used as catalysts and sorbents. For such materials, the loaded metal or metal oxide is commonly the active component of the catalysis and chemical adsorption. However their activity often exhibits considerable differences dependent on the dispersion and oxidation states of the metal species, especially when the metal is variable in valence state. Controlled synthesis of materials with dispersed pure phase metal or value-well-defined metal species is one of the essential topics in preparation of the materials.

Copper-supporting mesoporous silicas have been reported to be excellent catalysts for many redox reactions, such as the selective catalytic reduction of nitrous oxide with ammonia and methane,[1] the liquid-phase hydroxylation of benzene, phenol, and alkyl-substituted phenol with hydrogen peroxide,[2] the catalytic oxidation of aniline[3] and cyclohexane,[4] 1-butene skeletal isomerization,[5] the selective hydrogenation of furfural to furfuryl alcohol,[6] *etc*. They were also shown to be excellent gas desulfurization sorbents.[7] For these copper-containing materials, the conventional preparation methods can be classified as hydrothermal methods and post-synthesis modifications. The former are used to enclose Cu^{2+} in the framework of molecular sieves, while the latter, including wetness impregnation using aqueous solutions of copper salt and ion exchange with surface hydroxyl groups, are frequently used to load copper species (Cu–, Cu_2O–, CuO) on the pore surface. Recently, a metal–organic chemical vapor deposition (MOCVD) technique with organocopper complexes as precursors has been reported for preparation of highly dispersed metal copper or copper oxide on solid supports.[8] However, all these methods are ineffective for the controlled synthesis of copper species with a specific state due to the migration of copper ions from the inside to the outside of the framework for isomorphously copper-substituted molecular sieves [9] and the conglomeration of copper species on the surface of supports upon obligatory heat treatment. This leads to heterogeneous distribution of copper, and therefore makes identification of copper states difficult and understanding of nature of catalytic activity disputable.

In previous work, we studied the deposition chemistry of $Cu[OCHMeCH_2NMe_2]_2$ on surface of MCM-41.[10] It was revealed that the copper precursor can be adsorbed chemically on the surface of MCM-41 to form a stable surface copper complex coordinated with two framework oxygen atoms by ligand exchange at a temperature below 423 K. Since the copper atom of the surface complex is fixed in a specific position on the surface, it is possible to derive other well-defined copper species from the surface complex by post-treatment. Based on this consideration, we investigate in this paper the controlled preparation of pure Cu(II)/MCM-41, Cu(I)/MCM-41, and Cu(0)/MCM-41 with the surface organo-copper-supported on MCM-41 as precursor. The as-prepared copper-containing MCM-41 samples were shown to have relatively well-defined chemical states.

Experimental

Materials

$Na_2Si_3O_7$, dimethylamino-2-propanol, and Nano-CuO were purchased from Sigma-Aldrich, Merk-Schuchardt, and Alfa-Aesar,

State Key Laboratory Breeding Base of Photocatalysis, Research Institute of Photocatalysis, Fuzhou University, Fuzhou 350002, P. R. China. E-mail: xwang@fzu.edu.cn, xzfu@fzu.edu.cn; Fax: +86 591 83779251; Tel: +86 591 83779251

respectively. Both CO gas (99.95%) and NO gas (99.9%) were purchased from Linde Gas (Xiamen) Co., Ltd. Other reagents were provided by Sinopharm Chemical Reagent Co., Ltd. All of the reagents were used without further purification.

Preparation of materials

MCM-41 was synthesized by a typical hydrothermal procedure using tetradecyltrimethylammonium bromide as surfactant and $Na_2Si_3O_7$ as the source of silica followed by calcination under flowing oxygen at 813 K for 20 h.[11] $Cu[OCHMeCH_2NMe_2]_2$ was prepared by an alcohol-exchange reaction process described in the literature.[8b] The copper-containing MCM-41 title materials were prepared by reaction of $Cu[OCHMeCH_2NMe_2]_2$ with pretreated MCM-41 at 353 K followed by chemical treatment with O_2 oxidant or CO/He reducing agent. The preparation was performed in an *in situ* IR glass cell connected to a vacuum line. A bare MCM-41 wafer was first pretreated under dynamic vacuum (10^{-4} Torr) at 773 K for 4 h. When cooling to room temperature, a pentane solution containing a fixed amount of $Cu[OCHMeCH_2NMe_2]_2$ was introduced into the cell with a syringe *via* a septum. After removing the solvent at room temperature by evacuation, the system was then kept at 353 K for 10 h for the reaction. The resulting blue solid was subsequently treated to eliminate the physisorbed species under dynamic vacuum at the same temperature for 2 h. The final solid, $Cu[OCHMeCH_2NMe_2]_2$/MCM-41, had been characterized previously and denoted as SC1.[10] Cu(II)/MCM-41 was obtained by calcination of SC1 under a highly pure and dry oxygen atmosphere (66–80 kPa) at more than 573 K for 2 h. The two reduced samples, Cu(I)/MCM-41 and Cu(0)/MCM-41 were prepared by calcination of the Cu(II)/MCM-41 under a mixed CO–He atmosphere of 3.9 vol% CO in He. The preparation processes above were monitored by IR spectroscopy. A large amount of the samples used for other characterizations were prepared in a glass tube by the above procedure.

Methods used for characterization

X-Ray powder diffraction data were obtained on a Bruker D8 Advance X-ray diffractometer with Cu-Kα irradiation. The BET specific surface areas and pore size distributions were measured by N_2 adsorption at 77 K on a Micromeritics ASAP 2020. IR spectra were recorded in transmittance mode on a Nicolet Nexus 670 FTIR spectrometer with a DTGS detector. The sample was pressed into a self-supporting wafer of 10–15 mg and placed into a home-made glass cell with ZnSe windows, which allows work *in situ* at temperatures up to 773 K. As for NO or CO adsorption, the IR spectrum collected before gas dosage was used as background. All the reported spectra of NO (or CO) adsorption were background-subtracted. All spectra consist of 32 scans taken at 4 cm^{-1} resolution. Temperature-programmed reduction (TPR) was carried out on an Auto Chem 2920 (Micromeritics, USA) instrument. In a typical experiment, 100 mg of sample was pretreated in argon flow of 30 ml min^{-1} at 473 K for 2 h, and then cooled to room temperature. The TPR experiment was carried out from room temperature to 773 K in a flow of 10 vol% H_2–Ar mixture (30 ml min^{-1}) at a heating rate of 10 K min^{-1}. UV-Vis diffuse reflectance spectra (DRS) were recorded on a Varian 500 spectrometer referenced to $BaSO_4$ and were transformed into the Kubelka–Munk function, $f(R_\infty)$. Photoluminescence spectra (PL) were measured at room temperature by using an Edinburgh F-900 fluorescence spectrophotometer. X-Ray Photoelectron spectra (XPS) were measured on a Quantum 2000 spectrometer with mono-chromatised Al-Kα radiation ($h\nu$ = 1486.6 eV). Binding energies were corrected with the C1s line at 284.6 eV (accuracy within ± 0.2 eV). Background pressure during the data acquisition was kept below 10^{-10} bar.

Results and discussion

Preparation and characterization of Cu(II)/MCM-41

When $Cu[OCHMeCH_2NMe_2]_2$ is introduced to bare MCM-41 pretreated under dynamic vacuum (10^{-4} Torr) at 773 K for 4 h and then heating at 353 K, the organocopper precursor is chemically anchored on MCM-41 *via* the reaction of the surface hydroxyls with the organocopper precursor to form a seven-membered ring chelate Cu complex containing an intramolecular hydrogen bond, which was reported in our previous work.[10] In the present work, the resultant sample denoted as SC1 will be used as a precursor for preparation of the title samples. The SC1 is relatively stable in natural air at room temperature or in a vacuum below 423 K.[10] Fig. 1 shows the change in IR spectra of the SC1 sample with increasing temperature in an oxygen atmosphere of 600 Torr. It remains stable until 353 K (Fig. 1a). Upon increasing the temperature to 373 K, although the intensities of the C–H stretching and bending vibration bands in the wavenumber range of 3100–2700 cm^{-1} and 1500–1300 cm^{-1} slightly decrease, some weak absorptions at 1572, 1620, and 1652 cm^{-1} attributed to C═N, –OH and C═C groups begin to emerge (Fig. 1b), indicating the oxidation of the surface copper complex starting at such a temperature. In the temperature range 373–573 K, the intensity of the bands at 1572, 1620, and 1652 cm^{-1} undergoes a gradual increase and then a rapid decrease till they vanish, along with the gradual decay of C–H absorption and the re-appearance of the surface hydroxyls of MCM-41. Further increasing the temperature does not result in visible change in the IR spectrum. This shows that the organocopper supported on MCM-41 is oxidized by oxygen into Cu(II)/MCM-41 at 573 K, which will be validated by physicochemical characterizations later.

Fig. 2 shows the TPR profiles of the resulting Cu(II)/MCM-41 with pure CuO as a reference. It can be seen that the pure CuO exhibits a wide peak centered at 495 K with a shoulder at 507 K, while the as-prepared Cu(II)/MCM-41 sample shows a nearly symmetrical peak with no shoulder at 466 K. No reduction peak occurs at higher temperature for either sample, suggesting the complete reduction of Cu^{2+} to Cu^0 at these temperatures. For the pure CuO, the TPR peak with the shoulder could be a result of the two step reduction of Cu^{2+} ion to metallic copper: $Cu^{2+} \rightarrow Cu^{+} \rightarrow Cu^0$.[12] Fierro *et al.*,[13] however, reported that CuO reduces in only one step and the second signal, especially the shoulder, is an artefact originating from sublimation of metallic copper on the reduced CuO

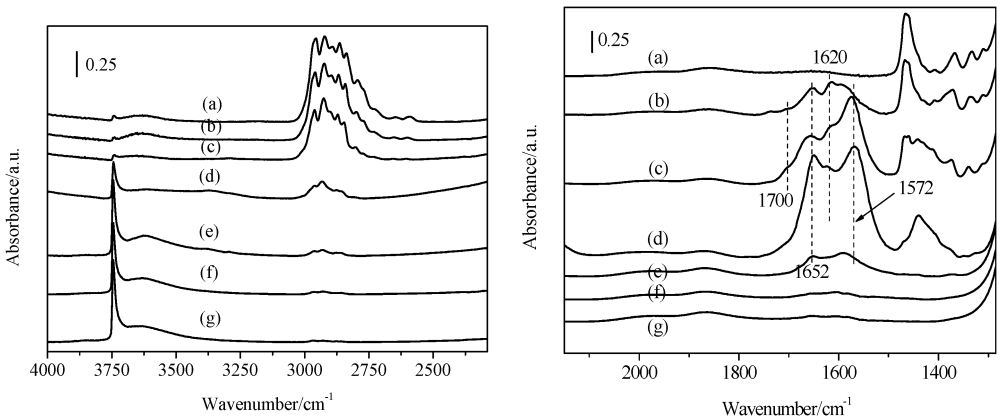

Fig. 1 Change in FT-IR spectra of the $Cu[OCHMeCH_2NMe_2]_2$ supported on MCM-41 under oxygen atmosphere with heating temperature: (a) 353 K, (b) 373 K, (c) 423 K, (d) 473 K, (e) 523 K, (f) 573 K, and (g) 623 K. It was evacuated at 323 K for 30 min after each treatment.

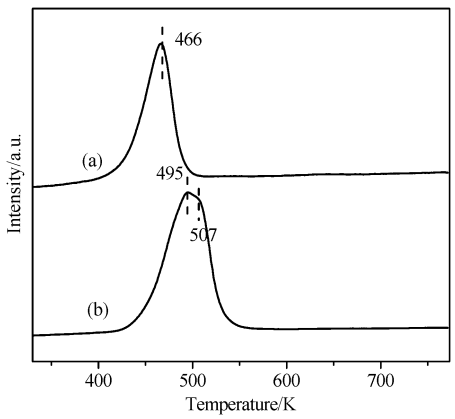

Fig. 2 H_2-TPR profile of (a) Cu(II)/MCM-41 and (b) pure CuO.

particles. For the Cu(II)/MCM-41, the single and symmetrical TPR peak occurring at lower temperature suggests high dispersivity of the Cu(II)–O species formed on the MCM-41 surface and therefore easier reduction to metal copper.[14]

The formed Cu(II)–O species in the as-synthesized sample are further identified by IR spectroscopy using NO as a probe molecule. Fig. 3 shows the IR spectra of samples after NO adsorption at room temperature. On increasing the NO pressure to 500 Pa, three visible absorption bands at 1882, 1610, and 1508 cm^{-1} and two weak bands at 1578 and 2130 cm^{-1} gradually emerge. The 1882 cm^{-1} band is admittedly assigned to the N–O bond stretching vibration in the Cu^{2+}–NO complex,[15] and the absence of any typical absorption band at 1775 cm^{-1} excludes the possibility of the presence of Cu^{+}.[16] The band at 1578 cm^{-1} is attributed to the monodentate nitrate species Cu(II)–O–NO_2, while the band at 1610 cm^{-1} is assigned to chelating bidentate nitrate Cu(II)O_2N–O. These two bands result from NO_2 molecules adsorbed on the isolated copper–oxygen species on the surface.[17] The formation of nitrate species is due to the equilibrium characteristic of NO: $3NO \leftrightarrow NO_2 + N_2O$.[18] The adsorption of NO on various solids often causes the formation of NO_x (x = 2, 3) without any evidence of reduction of the sample, which is usually explained by NO disproportionation and is accompanied by the formation of N_2O.[17] The weak absorption at 2130 cm^{-1} was reported to belong to the N–N stretching of N_2O adsorbed on copper-exchanged zeolite.[18] The strongest wide band at about 1508–1490 cm^{-1} has been rarely reported for other copper containing materials, which can be related to the special structure of the copper species in our sample. The assignment of this band is controversial in the literature. We speculate that it may belong to N–O stretches in nitrito (–O–N–O) or (–NO_2) complexes coordinated to Cu^{2+}, based on the wavenumber of the IR absorption.[17] No IR band at 1630 cm^{-1} attributed to the bridging bidentate nitrate $(CuO)_2$–N–O is observed,[17] indicating the absence of dimeric copper–oxo species in the sample. The above results show that pure Cu(II) supported on MCM-41 with isolated copper–oxo species is obtained by this route.

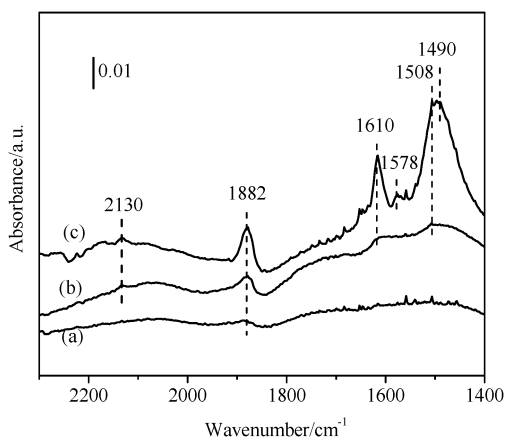

Fig. 3 IR spectra of Cu(II)/MCM-41 after adsorption of NO at room temperature under different NO pressures: (a) 10 Pa, (b) 100 Pa, (c) 500 Pa.

The above conclusion is also validated by characterization by diffuse reflectance spectroscopy. As shown in Fig. 4, the as-prepared Cu(II)/MCM-41 showed only a strong absorption peak at *ca.* 225 nm, which should be assigned to charge transfer between isolated Cu^{2+} ion and the oxygen ligand.[19] No significant absorption peak is observed above 300 nm, suggesting that the sample is free of copper oxide oligomers and big clustered copper species.[20] In contrast, the pure CuO as reference shows two broad absorption bands.

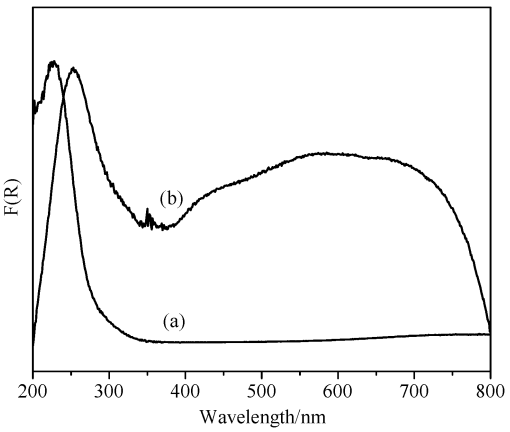

Fig. 4 UV-Vis DRS spectra of (a) Cu(II)/MCM-41 and (b) pure CuO.

All the results reported above show that the pure and highly dispersed Cu(II)–O-supporting MCM-41 sample has been prepared by calcination of $Cu[OCHMeCH_2NMe_2]_2$/MCM-41 in dry oxygen at 573 K for 2 h.

Preparation and characterization of Cu(I)/MCM-41 and Cu(0)/MCM-41

Metal copper (Cu^0) and cuprous oxide supported on MCM-41 could be obtained by further treatment of the as-prepared Cu(II)/MCM-41 sample under CO/He of *ca.* 60 kPa at a controlled temperature. Copper(I) oxides are the only copper oxides that can be identified by photoluminescence spectroscopy,[21] so we chose it first to characterize the products obtained by the reduction process.

Fig. 5 shows change in the photoluminescence emission spectra of sample with increasing temperature under CO/He atmosphere, upon excitation with 350 nm light. For the sample Cu(II)/MCM-41, no PL peak is observed (Fig. 5a). According to the study by Borgohain and Mahamuni, single-phase CuO nanoparticles were non-luminescent at room temperature.[22] No photoluminescence is additional evidence for the presence of only Cu^{2+} on the sample. Upon increasing the temperature to 473–573 K, the sample exhibits a wide PL band centered at *ca.* 440 nm with two shoulders at 410 and 480 nm. These peaks in the range 400–600 nm result from the characteristic electronic transitions $d^{10} \leftrightarrow d^9s^1$ of Cu^+ ions, indicating that the reduction of Cu^{2+} to Cu^+ occurs at 473–573 K. These peaks were also observed for the Cu(I) supported SiO_2, Al_2O_3, and zeolite.[23–25] When the heating temperature increases to above 573 K, the PL bands rapidly decrease in intensity and even disappear (Fig. 5d), indicating the complete reduction of Cu^+ to Cu^0 showing no fluorescence. According to the literature,[25,26] the peaks at 410 and 440 nm are ascribed to isolated Cu^+–O species with C_{3v} and C_{2h} ligand field symmetry, respectively. As for the emission at 480 nm, similar to Cu^+ ions located in close proximity to the two framework Al atoms in Cu^+/ZSM-5,[27] it was probably due to a type of Cu^+ site in a constricted structure. Since the strongest photoluminescence occurs at 473 K, it was reasonably concluded that the sample obtained at 473 K contains only isolated Cu^+–O species. The result also shows that the sample reduced at 673 K contains only pure copper metal in view of the absence of photoluminescence.

In order to further ensure the purity of the obtained samples, the Cu(II)/MCM-41 sample and the three samples reduced at 473, 573, and 673 K were further characterized by XPS. As shown in Fig. 6, the binding energy of Cu $2p_{3/2}$ of Cu in Cu(II)/MCM-41 is 934.6 eV, consistent with that of CuO or $Cu(OH)_2$, and a shake-up satellite peak is observed in the binding energy range 940–950 eV, confirming further that copper exists as Cu^{2+} ions.[28] For pure CuO, the Cu $2p_{3/2}$ binding energy is 933.6 eV; the shift toward higher energy is indicative of charge transfer from the copper(II) ion to the support.[29] Therefore, the interaction of well-dispersed Cu^{2+} with the silica surface occurs for Cu(II)/MCM-41. For pure and uniform Cu^{2+} ions, the intensity ratio of the satellite to the $2p_{3/2}$ peak is ordinarily 0.5.[30] For our Cu(II)/MCM-41 sample the ratio close to 0.5 further indicates that pure Cu(II)–O species are present in the sample. For the sample reduced at 473 K, the satellite peak completely disappears and the main line shifts to 932.6 eV (Fig. 6b). Further increasing the reaction temperature from 573 to 673 K leads to the shift of the Cu $2p_{3/2}$ peak to 932.4 eV (Fig. 6c and d), indicating further reduction of the copper species. Unfortunately, Cu^0 cannot be distinguished from Cu^+ by the Cu 2p XPS spectra

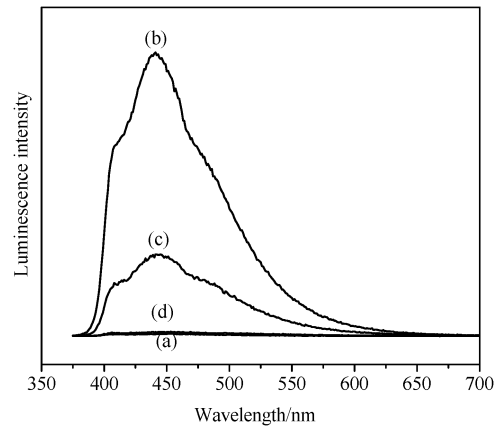

Fig. 5 Photoluminescence spectra of (a) Cu(II)/MCM-41, and Cu(II)/MCM-41 reduced under CO/He atmosphere at (b) 473 K, (c) 573 K, and (d) 673 K.

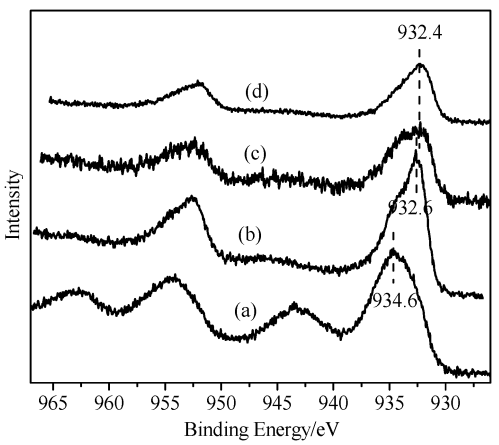

Fig. 6 XPS spectra of Cu 2p of (a) Cu(II)/MCM-41, and Cu(II)/MCM-41 reduced under CO/He at (b) 473 K, (c) 573 K, and (d) 673 K.

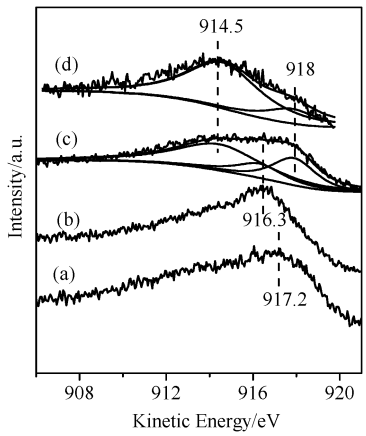

Fig. 7 XPS spectra of Cu LMM of (a) Cu(II)/MCM-41, and Cu(II)/MCM-41 reduced under CO/He at (b) 473 K, (c) 573 K, and (d) 673 K.

because of their spectral overlap.[31] Thus further characterization was carried out by Cu $L_3M_{4,5}M_{4,5}$ Auger spectra. As shown in Fig. 7, for the Cu(II)/MCM-41 sample the kinetic energy of Cu LMM is observed at 917.2 eV (Fig. 7a), typical for the kinetic energy of Cu^{2+}.[30] It is entirely consistent with the result from Cu 2p XPS. As the reduction temperature increases to 473 K, the main peak shifts to 916.3 eV (Fig. 7b), which is characteristic of Cu^+, indicating the formation of pure Cu(I)–O species in the sample.[32] However for the sample reduced at 573 K, the Auger spectra exhibit a broadening peak, which can be divided into three peaks centered at 916.3, 918, and 914.5 eV (Fig. 7c) by gaussian fitting. According to the literature, the peak with a kinetic energy of 918 eV is attributed to metallic copper,[32] while the peak at 916.3 eV is assigned to Cu(I). As for the peak at 914.5 eV, it can be also related to Cu metal,[33] although it is not always useful for chemical state determination.[34] It indicates the coexistence of cuprous oxide and metallic copper at 573 K. Interestingly, the peak at 916.3 eV disappears at 673 K (Fig. 7d) but the two peaks at 918 and 914.5 eV remain in their existing state, suggesting the presence of pure copper metal on the surface at 673 K. These results were in good agreement with that of the PL spectra.

The states of copper in the two reduced samples were also characterized by IR spectroscopy using CO as a probe molecule. Changes in the IR spectra of samples reduced at 473 K and 673 K with increasing pressure of CO are shown in Fig. 8(A) and (B), respectively. For the sample reduced at 473 K, a single band is observed at 2129 cm^{-1} with increasing CO pressure. This band is typically ascribed to Cu^+–CO species,[15,35] showing that copper species are present in the form of Cu(I) for the sample reduced at 473 K. As for the sample reduced at 673 K, the absorption of CO occurs at 2112 cm^{-1}rather than 2129 cm^{-1} (Fig. 8B(a)). The bands near 2110 cm^{-1} are often attributed to either Cu^+–CO or Cu^0–CO species in the literature,[36] but both species could be distinguished by the absorption strength.[15] The CO molecule forms mainly a π-bond complex with a Cu^0 atom, and the resulting complex is unstable and therefore CO is easily desorbed upon evacuation.[15] As shown in Fig. 8B(d), since the band completely disappears upon evacuation at room temperature, the IR band should belong to Cu^0–CO species rather than Cu^+–CO species, *i.e.* the sample reduced at 673 K only contains metallic copper on the surface.

The crystalline structure of the as-prepared samples was characterized by XRD, as shown in Fig. 9. No major change in the structure of MCM-41 is observed after copper modification. It indicates that these post-treatment processes, including calcination and reduction, do not destroy the mesoporous structure of the support MCM-41. At low angle all samples exhibit a main peak at 2.2° indexed as [100] due to a hexagonal array of parallel mesoporous tubes. The supporting of Cu(II)–O species and the subsequent reduction treatment cause merely a little decrease in the intensity of all diffraction peaks, reflecting a decrease in the ordering of the hexagonal pore structure. No additional reflections of crystalline cuprous oxide and copper metal are observed from the XRD pattern at high angle (not shown) after the reduction of the Cu(II)/MCM-41 in CO/He at *ca.* 60 kPa atmosphere. It originates from the low copper content of *ca.* 1.5 wt%, which is below the detection limit of XRD analysis.

The N_2 adsorption characterization of the as-synthesized samples is shown in Fig. 10 and the results are summarized in Table 1. The copper modification results in a decrease in the amount of nitrogen adsorbed (corresponding to the loss of surface area), but all the samples retain a typical type IV isotherm (IUPAC classification). It further validates that the reduction process does not destroy the mesoporous structure of the MCM-41 support. The obatined Cu(II)/MCM-41 sample has the almost same BJH pore diameter as bare MCM-41, indicating that the supported Cu(II)–O species should be uniformly dispersed on the support surface. The Cu(I)/MCM-41 and Cu(0)/MCM-41 obtained after reduction have a smaller BJH pore diameter of *ca.* 2.85 nm, and moreover, the reduction treatment leads to a consequent decrease in BET surface area, as a result of carbon deposits formed during reduction. These carbon deposits visibly change the color of the reduced samples to black.

All of the characterization results reported above indicate that after calcining the $Cu[OCHMeCH_2NMe_2]_2$/MCM-41 under oxygen atmosphere at 573 K, the Cu(II)–O species obtained is highly isolated. Scheme 1 shows the possible formation route of Cu(II), Cu(I), and Cu(0) on the MCM-41 surface. These Cu(II)–O and Cu(I)–O species obtained could be easily hydrated to $Cu(OH)_2$ and CuOH surface phases, as a result of the formation of H_2O during calcination. The chelation of the center copper atom with the organic ligand oxygen atoms and the silanol groups of the MCM-41 support prevents copper from aggregating into Cu(II)–O clusters or large particles. Most of the Cu^{2+} and Cu^+ is highly dispersed on the surface of MCM-41 in the form of $Cu(OH)_2$ and CuOH, respectively, after calcination. The high dispersity can enhance the reducibility of Cu(II)–O species compared to bulk CuO particles, as shown by the TPR results. Under a limited supply of CO, these highly isolated Cu(II)–O species are reduced to Cu(I)–O species or metallic copper by controlling the reaction temperature. The Cu(I)–O species and metallic copper still are highly dispersed on the inner wall

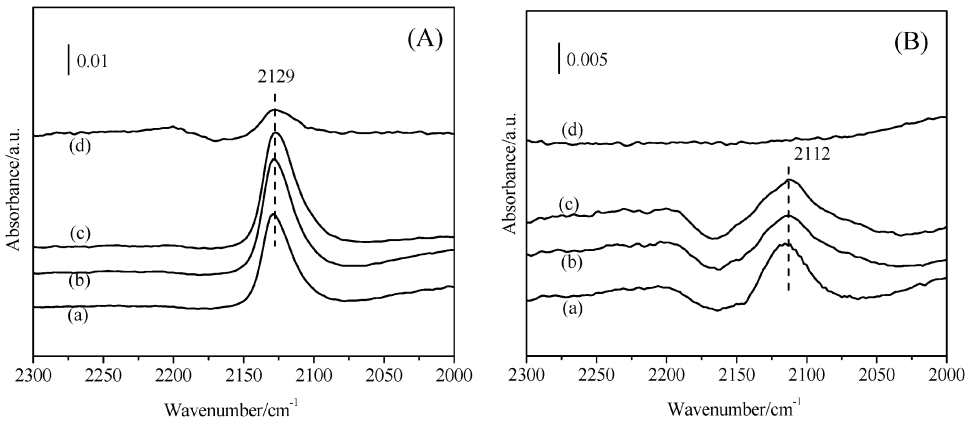

Fig. 8 Change in the IR spectra of CO adsorption on the Cu(II)/MCM-41 reduced at (A) 473 K and (B) 673 K with CO pressure: (a) 150 Pa, (b) 200 Pa, (c) 250 Pa, (d) upon evacuation at ambient temperature.

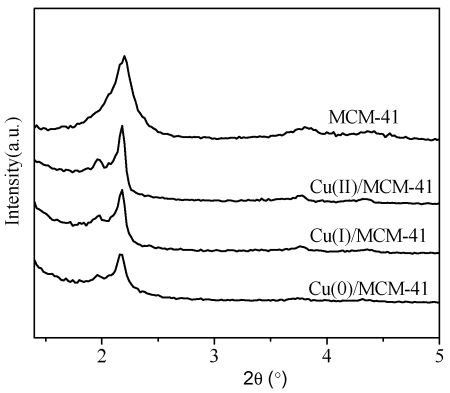

Fig. 9 XRD patterns of as-prepared samples.

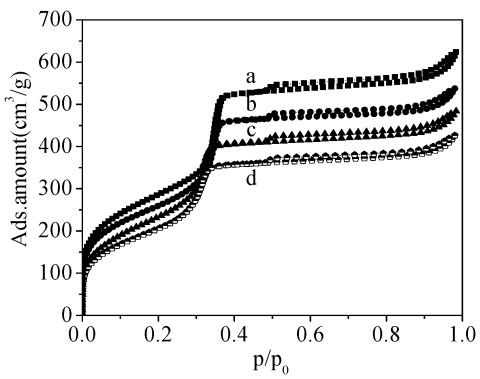

Fig. 10 Nitrogen adsorption–desorption isotherms of the synthesized samples: (a) Cu(II)/MCM-41, and Cu(II)/MCM-41 reduced at (b) 473 K, (c) 673 K.

surfaces of MCM-41. The MCM-41 support makes a certain contribution to the stable presence of Cu(II), Cu(I), Cu(0) isolated sites by coordination.

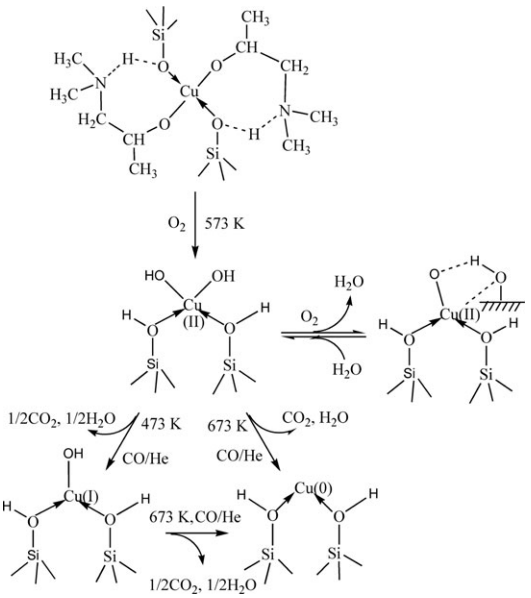

Scheme 1 Formation of Cu(II), Cu(I), and Cu(0)/MCM-41.

Conclusions

Pure copper oxide, cuprous oxide, and metallic copper supported on MCM-41 could be obtained by the thermal treatment of $Cu[OCHMeCH_2NMe_2]_2$/MCM-41 under O_2 and CO/He atmosphere at a controlled temperature, respectively. Calcination of $Cu[OCHMeCH_2NMe_2]_2$/MCM-41 at 573 K in pure O_2 led to the formation of Cu(II)/MCM-41. Cu(I)/MCM-41 could be obtained from Cu(II)/MCM-41 by calcination at 473 K under CO/He atmosphere, while the Cu(0)/MCM-41 was prepared under the same conditions but at 673 K. Physicochemical characterization suggested that the Cu(II)–O, Cu(I)–O and metallic Cu species are highly dispersed

Table 1 Surface area, copper content, and BJH pore diameter of the synthesized copper supported samples

Sample	Copper content (wt%)	S_{BET}/m^2g^{-1}	BJH pore diameter/nm
MCM-41	0.00	1047	3.01
Cu(II)/MCM-41	1.54	971.1	2.97
Cu(I)/MCM-41	1.49	906.4	2.87
Cu(0)/MCM-41	1.60	834.6	2.83

on the surface of MCM-41 and present in the isolated states. The Cu(II)–O species highly dispersed on the surface of MCM-41 materials are expected to be able to enhance considerably the catalytic activity for phenol hydroxylation.

Acknowledgements

This work was financially supported by the National Science Foundation of China (No. 20673020, 20873022, 20537010), National Basic Research Program of China (973 Program 2007CB613306), Special subjects of National High Technology Development Program of China (863 Program 2008AA06Z326).

References

1 (*a*) L. Chmielarz, P. Kutrowski, M. Kruszec, R. Dziembaj, P. Cool and E. Vansant, *J. Porous Mater.*, 2005, **12**, 183; (*b*) C. C. Liu and H. Teng, *Appl. Catal., B*, 2005, **58**, 69; (*c*) Y. Wan, J. Ma, Z. Wang, W. Zhou and S. Kaliaguine, *J. Catal.*, 2004, **227**, 242.
2 (*a*) Z. H. Sun, L. F. Wang, P. P. Liu, B. Sun, D. Z. Jiang and F. S. Xiao, *Chin. J. Chem.*, 2006, **24**, 1653; (*b*) L. L. Lou and S. Liu, *Catal. Commun.*, 2005, **6**, 762; (*c*) L. N. Franco, I. H. Perez, J. A. Pliego and A. M. Franco, *Catal. Today*, 2002, **75**, 189; (*d*) Z. Fu, J. Chen, D. Yin, D. Yin, L. Zhang and Y. Zhang, *Catal. Lett.*, 2000, **66**, 105; (*e*) L. Wang, A. Kong, B. Chen, H. Ding, Y. Shan and M. He, *J. Mol. Catal. A: Chem.*, 2005, **230**, 143; (*f*) H. Fujiyama, I. Kohara, K. Iwai, S. Nishiyama, S. Tsuruya and M. Masaic, *J. Catal.*, 1999, **188**, 417.
3 H. T. Gomesa, P. Selvamc, S. E. Dapurkarc, J. L. Figueiredoa and J. L. Faria, *Microporous Mesoporous Mater.*, 2005, **86**, 287.
4 W. A. Carvalhoa, M. Wallaub and U. Schuchardt, *J. Mol. Catal. A: Chem.*, 1999, **144**, 91.
5 V. Nieminen, N. Kumar, J. Datka, J. Paivarinta, M. Hotokka, E. Laine, T. Salmi and D. Y. Murzin, *Microporous Mesoporous Mater.*, 2003, **60**, 159.
6 X. Y. Hao, W. Zhou, J. W. Wang, Y. Q. Zhang and S. Liu, *Chem. Lett.*, 2005, **34**, 1000.
7 (*a*) O. Karvan and H. Atakül, *Fuel Process. Technol.*, 2008, **89**, 908; (*b*) Z. Ozaydin, S. Yasyerli and G. Dogu, *Ind. Eng. Chem. Res.*, 2008, **47**, 1035; (*c*) Y. Wang, R. T. Yang and J. M. Heinzel, *Ind. Eng. Chem. Res.*, 2009, **48**, 142.
8 (*a*) V. N. Vertoprakhov and S. A. Krupoder, *Russ. Chem. Rev.*, 2000, **69**, 1057; (*b*) S. C. Goel, K. S. Kramer, M. Y. Chiang and W. E. Buhro, *Polyhedron*, 1990, **9**, 611; (*c*) V. L. Young, D. F. Cox and M. E. Davis, *Chem. Mater.*, 1993, **5**, 1701; (*d*) R. Becker, A. Devi, H. W. Becker and R. A. Fischer, *Chem. Vap. Deposition*, 2003, **9**, 149; (*e*) R. Becker, H. Parala, F. Hipler, O. P. Tkachenko, K. V. Klementiev, W. Grünert, H. Wilmer, O. Hinrichsen, M. Muhler, A. Birkner, C. Wöll, S. Schäfer and R. A. Fischer, *Angew. Chem., Int. Ed.*, 2004, **43**, 2839; (*f*) L. Lu, A. Wohlfart, H. Parala, A. Birkner and R. A. Fischer, *Chem. Commun.*, 2003, 4.
9 P. Fejes, J. B. Nagy, K. Lázár and J. Halász, *Appl. Catal., A*, 2000, **190**, 117.
10 G. Zhang, X. Wang, J. Long, L. Xie, Z. Ding, L. Wu, Z. Li and X. Fu, *Chem. Mater.*, 2008, **20**, 4565.
11 X. X. Wang, F. Lefebvre, J. Patarin and J. M. Basset, *Microporous Mesoporous Mater.*, 2001, **42**, 269.
12 S. J. Gentry, N. W. Hurst and A. Jones, *J. Chem. Soc., Faraday Trans. 1*, 1981, **77**, 603.
13 G. Fierro, M. L. Jacono, M. Inversi, G. Moretti, P. Porta and R. Lavecchia, *Proceedings of the 10th International Congress on Catalysis*, Budapest, 1992.
14 (*a*) S. J. Gentry and P. T. Walsh, *J. Chem. Soc., Faraday Trans. 1*, 1982, **78**, 1515; (*b*) A. Wollner, F. Lange, H. Schmeldz and H. Knozinger, *Appl. Catal., A*, 1993, **94**, 181.
15 K. Hadjiivanov and H. Knözinger, *Phys. Chem. Chem. Phys.*, 2001, **3**, 1132.
16 S. Bordiga, C. Pazé, G. Berlier, D. Scarano, G. Spoto, A. Zecchina and C. Lamberti, *Catal. Today*, 2001, **70**, 91.
17 I. Sobczak, M. Ziolek, M. Renn, P. Decyk, I. Nowak, M. Daturi and J.-C. Lavalley, *Microporous Mesoporous Mater.*, 2004, **74**, 23.
18 K. Hadjiivanov, *Catal. Rev. Sci. Eng.*, 2000, **42**, 71.
19 (*a*) T. Komatsu, M. Nunokawa, I. S. Moon, T. Takahara, S. Namba and T. Yashima, *J. Catal.*, 1994, **148**, 427; (*b*) R. A. Schoonheydt, *Catal. Rev. Sci. Eng.*, 1993, **35**, 129.
20 (*a*) M. R. Prasad, G. Kamalakar, S. J. Kulkarni and K. V. Raghavan, *J. Mol. Catal. A: Chem.*, 2002, **180**, 109; (*b*) M. C. Marison, E. Garbowski and M. Primet, *J. Chem. Soc., Faraday Trans.*, 1990, **86**, 3027; (*c*) M. Shimokawabe, N. Takezawa and H. Kobayashi, *Appl. Catal.*, 1982, **2**, 379.
21 N. Bellakhal, K. Draou, B. G. Chieron and J. L. Brisset, *Mater. Sci. Eng., B*, 1996, **41**, 206.
22 K. Borgohain and S. Mahamuni, *J. Mater. Res.*, 2002, **17**, 1220.
23 M. Anpo, M. Matsuoka, Y. Shioya, H. Yamashita, E. Giamello, C. Morterra, M. Che, H. H. Patterson, S. Webber, S. Ouellette and M. A. Fox, *J. Phys. Chem.*, 1994, **98**, 5744.
24 J. Dědeček, Z. Sobalík, Z. Tvarůžková, D. Kaucký and B. Wichterlová, *J. Phys. Chem.*, 1995, **99**, 16327.
25 (*a*) J. D. Barrie, B. Dunn, G. Hollingsworth and J. I. Zink, *J. Phys. Chem.*, 1989, **93**, 3958; (*b*) K. S. Shin, J. D. Barrie, B. Dunn and J. I. Zink, *J. Am. Chem. Soc.*, 1990, **112**, 5701.
26 T. Kurobori, S. Taniguchi and N. Takeuchi, *J. Lumin.*, 1993, **55**, 183.
27 J. Dědeček and B. Wichterlová, *J. Phys. Chem.*, 1994, **98**, 5721.
28 Y. Wan, J. Ma, Z. Wang, W. Zhou and S. Kaliaguine, *Appl. Catal., B*, 2005, **59**, 235.
29 J. Huang, S. Wang, X. Guo, D. Wang, B. Zhu and S. Wu, *Catal. Commun.*, 2008, **9**, 2131.
30 A. Tschöpe, M. L. Trudeau and J. Y. Ying, *J. Phys. Chem. B*, 1999, **103**, 8858.
31 C.-K. Wu, M. Yin, S. O'Brien and J. T. Koberstein, *Chem. Mater.*, 2006, **18**, 6054.
32 J. P. Espinós, J. Morales, A. Barranco, A. Caballero, J. P. Holgado and A. R. González-Elipe, *J. Phys. Chem. B*, 2002, **106**, 6921.
33 (*a*) S. Y. Lee, N. Mettlach, N. Nguyen, Y. M. Sun and J. M. White, *Appl. Surf. Sci.*, 2003, **206**, 102; (*b*) H. D. Speckmann, S. Haupt and H.-H. Strehblow, *Surf. Interface Anal.*, 1988, **11**, 148; (*c*) C. E. Dubé, B. Workie, S. P. Kounaves, A. Robbat and M. L. Aksu, *J. Electrochem. Soc.*, 1995, **142**, 3357.
34 L. Burzyńska, *Corros. Sci.*, 2001, **43**, 1053.
35 (*a*) M. Iwamoto and Y. Hoshino, *Inorg. Chem.*, 1996, **35**, 6918; (*b*) K. Hadjiivanov, T. Tsoncheva, M. Dimitrov, C. Minchev and H. Knözinger, *Appl. Catal., A*, 2003, **241**, 331.
36 (*a*) G. Busca, *J. Mol. Catal.*, 1987, **43**, 225; (*b*) A. Dandekar and M. A. Vannice, *J. Catal.*, 1998, **178**, 621; (*c*) V. Indovina, M. Occhiuzzi, D. Pietrogiacomi and S. Tuti, *J. Phys. Chem. B*, 1999, **103**, 9967.

